Application of Chebyshev neural network to solve Van der Pol equations

Sarkhosh S. Chaharborj[1]*, Shahriar S. Chaharborj[2] and Phang Pei See[3]

[1]*School of Mathematics and Statistics, Carleton University, Ottawa, K1S 5B6, Canada*
[1]*Department of Mathematical Sciences, Faculty of Science, Universiti Teknology Malaysia, 81310 UTM Johor darul Takzim, Malaysia*
[2]*Department of Mathematics, Tabriz Branch, Islamic Azad University, Tabriz, Iran*
[3]*Department of Mathematics, Faculty of Science, Universiti Putra Malaysia, 43400 UPM, Malaysia*
[3]*Brilliant Student Care 838, Jurong West Street 81 640838, Singapore*
*Corresponding author E-mail: sseddighi2014@yahoo.com.my & saman.seddighi@carleton.ca

Abstract

In dynamics, the Van der Pol oscillator is a non-conservative oscillator with non-linear damping. The problems of single-well, double-well and double-hump Van der Pol-Dufing equations are studied in this paper. The Chebyshev Neural Network (ChNN) model will be applied to obtain the numerical solutions of these types of equations for the first time. The hidden layer is eliminated by expanding the input pattern by Chebyshev polynomials which employs a single layer neural network. In order to modify the network parameters and to minimize the computed error function, a feed forward neural network model with error back propagation principle is used. The obtained numerical results form the ChNN model will be compared with the analytical solutions, namely Homotopy Perturbation Method (HPM), Homotopy Analysis Method (HAM), Differential Transform Method (DTM) and exact. Comparisons of the solutions obtained with existing numerical results show that this method is a capable tool for solving this kind of nonlinear problems.

Keywords: *Van der Pol equations; Chebyshev Neural Network; Error back propagation algorithm; Feed forward neural network.*

1. Introduction

The Van der Pol oscillator is a basic model of the oscillation theory and nonlinear dynamics, which describes self-oscillations and the simplest version of the Andronov-Hopf bifurcation. The Van der Pol oscillator is named after a Dutch scientist, Balthasar Van der Pol who established experimental results on the dynamics of an oscillator in electrical circuits governed by a second order differential equation [1]. This equation has been used for modelling oscillatory phenomenon in engineering, physics, biology, neurology, chemical reactions even in economics. Therefore, it is of utmost importance to develop a faster and more accurate solutions to solve the Van der Pol oscillator are very importance.

An analytical solution for Van der Pol-Duffing oscillators has been provided by Kimiaeifar et al. by homotopy analysis method [2]. The author also provided an analytical solution of modify Van der Pol's oscillator using He's parameter-expanding methods [3]. Khan et al. proposed a scheme that depends on two component of the homotopy series which is the Laplace transformation and the Pade approximate to obtain the solution for the force-free Duffing Van der Pol oscillator equations [4]. Besides that, Liao's homotopy analysis method has been used by Chen and Liu to study the Duffing Van der Pol equation [5].

There are several numerical methods studied by researchers to approximate the solution of the Van der Pol Duffing oscillator. Molaei and Kheybari provided an approximate solution of the the Van der Pol Duffing oscillator using the parameter expansion method and compared it with the perturbation method [6]. Motsa and Sibanda presented a novel application of the successive linearisation method to the Van der Pol duffing oscillator equations [7]. A differential transformation method has been implemented to study the Van der Pol duffing oscillator equation [8, 9, 10, 11]. Soomro et al. investigated and compared among improved Heun's method, Runge-Kutta order fourth and mid-point method to show that the Runge-Kutta method can obtain better accuracy compare to the Heun and mid-point method [12]. Dynamical analysis of two coupled parametrically excited Van der Pol oscillators presented by Qinsheng in 2004 [13]; a novel harmonic balance analysis for the Van der Pol oscillator has been studied by Liu et al. in 2007 [14]; fast parametrically excited Van der Pol oscillator with time delay state feedback has been provided by Belhaq and Sah in 2008 [15]; discontinuous synchrony in an array of Van der Pol oscillators have been provided by Perlikowski et al. in 2010 [16]; Ramana and Prasad in 2014 proposed modified Adomian Decomposition method for analyzing Van der Pol equations [17].

The general case of Van der Pol driven equations [17] is as follows,

$$m(t,u,u')\frac{\partial^2 u}{\partial t^2} + c(t,u,u')\frac{\partial u}{\partial t} + k_1(t,u)u + k_2(t,u)u^3 = F\cos(\omega t), \tag{1}$$

with assumptions that mass $m = 1$, damping coefficient $c' = \mu(c - bu^2)$, stiffness $k_1 = k_2 = 1$ and drive forcing $F = F\cos(\omega t)$, therefore the equations(1) yields to dampen the second order inhomogeneous equation as follows,

$$\frac{d^2 u}{dt} + \mu(c - bu^2)\frac{du}{dt} + u + u^3 = F\cos(\omega t); \quad t \geq 0, \tag{2}$$

with initial conditions $u(0) = a_1$ and $u'(0) = a_2$.

In this paper, we attempt to solve the Van der Pol duffing equation using the Chebyshev neural network method with a single layer and eliminate hidden layers by expanding the input pattern using Chebyshev polynomials. To minimize the computed error function a feed forward neural network model with an error back propagation principle is used.

2. Methods

The structure of a single layered Chebyshev neural network (ChNN) model and learning algorithm will be introduced in this section.

2.1. Structure of Chebyshev neural network model

Fig. (1) shows the structure of the Chebyshev Neural Network (ChNN) [18] which consists of single input unit, one output unit and a functional expansion block based on Chebyshev polynomials [19, 20]. The ChNN model is a single layer neural model where each input data is expanded to several terms using Chebyshev polynomials. In this paper, we used a one input node only. The first two Chebyshev polynomials are,

$$\begin{aligned} T_0(x) &= 1, \\ T_1(x) &= x. \end{aligned}$$

The higher order Chebyshev polynomials may be evaluated by the following formula,

$$T_{n+1}(x) = 2xT_n(x) - T_{n-1}(x), \tag{3}$$

where $T_n(x)$ denotes the n-th order Chebyshev polynomial. Here the n dimensional input pattern is expanded to m dimensions enhanced by Chebyshev polynomials. The advantage of the ChNN is get results using a single layer network by increasing the dimension of the input through Chebyshev polynomial [19, 20]. The architecture of the network with the first m Chebyshev polynomials and single input and output layer is shown in Fig. (1).
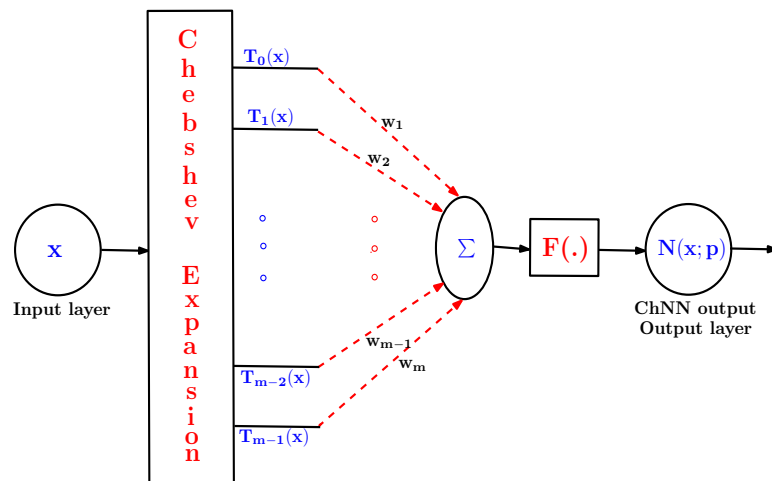
Figure 1: Structure of single layer Chebyshev Neural Network.

2.2. Learning algorithm of Chebyshev neural network

For updating the network parameters and minimizing the error function, the learning algorithm can be employed. To update the weights of the ChNN, the error back propagation algorithm is used. In order to achieve that, the gradient of an error function with respect to the network parameters p is determined [19, 20]. Functions `F(z)=z; sinh(z); tanh(z)` are considered as the activation functions. The network output with input data x and parameters (weights) p may be computed as,

$$N(x,p) = F(z), \tag{4}$$

where z is the weighted sum of the expanded input data, written as follows,

$$z = \sum_{j=1}^{M} w_j T_{j-1}(x), \tag{5}$$

where x is the input data, $T_{j-1}(x)$ and w_j with $j = 1, 2, ..., M$ denote the expanded input data and the weight vector respectively of the Chebyshev Neural Network.

Now, the weights of the ChNN may be modified using the principle of back propagation [19, 20],

$$w_j^{k+1} = w_j^k + \Delta w_j^k = w_j^k + \left(-\eta \left[\frac{\partial E(x, p)}{\partial w_j} \right]^k \right), \tag{6}$$

where η is the learning parameter, k is the iteration step which is used to update the weights as usual in ANN and $E(x, p)$ is the error function.

3. Formulation of the method

In this section, general formulation of differential equations using the Neural Network have are described. In particular the formulations of ordinary differential equations (ODEs) are incorporated in detail with computation of the gradient of the network parameters with respect to its inputs [19, 20].

3.1. Chebyshev neural network formulation for differential equations

A general differential equation which represents ordinary or partial differential equations is as follows,

$$\Psi \left[x, y(x), \nabla y(x), \nabla^2 y(x), ..., \nabla^n y(x) \right] = 0, \quad x \in \bar{D} \subseteq R^n, \tag{7}$$

where Ψ is the function which defines the structure of differential equation, $y(x)$ and ∇ denotes the solution and differential operator, respectively. Let $y_t(x, p)$ denote the trial solution with adjustable parameters p, which will then cause the general differential equation above to changes to the form,

$$\Psi \left[x, y_t(x, p), \nabla y_t(x, p), \nabla^2 y_t(x, p), ..., \nabla^n y_t(x, p) \right] = 0, \tag{8}$$

The problem is transformed into the following minimization problem [19, 20, 21],

$$\min_p \frac{1}{2} \left[\sum_{x \in \bar{D}} \left[\Psi \left(x, y_t(x, p), \nabla y_t(x, p), \nabla^2 y_t(x, p), ..., \nabla^n y_t(x, p) \right) \right] \right]. \tag{9}$$

Now, we consider the second order ordinary differential equation (ODE) as follows,

$$\frac{d^2 y(x)}{dx^2} = f(x, y, y'); \quad x \in [a, b] \tag{10}$$

with the initial conditions, $y(a) = A$ and $y'(a) = A'$, with the trial solution $y_t(x, p)$ of the feed forward neural network with input x and parameters p written as,

$$y_t(x, p) = A + A'(x - a) + (x - a)^2 N(x, p). \tag{11}$$

Where, `N(x, p)=z; sinh(z); tanh(z)` and the general form of corresponding error function for the ODE's formula as stated in [19, 20],

$$E(x, p) = \sum_{i=1}^{n} \frac{1}{2} \left[\frac{d^2 y_t(x_i, p)}{dx^2} - f(x_i, y_t(x, p), y_t'(x, p)) \right]. \tag{12}$$

To minimize the error function $E(x, p)$ corresponding to every entry x, we differentiate $E(x, p)$ with respect to the parameters. Thereafter, the gradient of network output with respect to their inputs is computed as below.

3.2. Computation of gradient for optimizing values of weight

The error computation involves both output and derivatives of the network output with respect to the corresponding inputs [19, 20]. Subsequently, the gradient of network output with respect to their inputs for `N(x, p)=z; sinh(z); tanh(z)` is computed as stated below.

- **In the case of $N(\mathbf{x}, \mathbf{p}) = \mathbf{z}$:**
  Derivatives of $N(x, p) = z$ with respect to input x is as follows,

$$\frac{dN}{dx} = \sum_{j=1}^{M} w_j T'_{j-1}(x), \tag{13}$$

  and

$$\frac{d^2 N}{dx^2} = \sum_{j=1}^{M} w_j T''_{j-1}(x). \tag{14}$$

- **In the case of $N(x,p) = \sinh(z)$** :
  Derivatives of $N(x,p) = sinh(z)$ with respect to input x is as follows,

$$\frac{dN}{dx} = \frac{1}{2}\sum_{j=1}^{M} w_j T'_{j-1}(x) \left(e^{\sum_{j=1}^{M} w_j T_{j-1}(x)} + e^{-\sum_{j=1}^{M} w_j T_{j-1}(x)} \right),\tag{15}$$

and

$$\frac{d^2N}{dx^2} = \frac{1}{2}\left[\begin{array}{c} \sum_{j=1}^{M} w_j T''_{j-1}(x) e^{\sum_{j=1}^{M} w_j T_{j-1}(x)} + \left(\sum_{j=1}^{M} w_j T'_{j-1}(x) \right)^2 e^{\sum_{j=1}^{M} w_j T_{j-1}(x)} \\ + \frac{\sum_{j=1}^{M} w_j T''_{j-1}(x)}{e^{\sum_{j=1}^{M} w_j T_{j-1}(x)}} - \frac{\left(\sum_{j=1}^{M} w_j T'_{j-1}(x) \right)^2}{e^{\sum_{j=1}^{M} w_j T_{j-1}(x)}} \end{array} \right].\tag{16}$$

- **In the case of $N(x,p) = \tanh(z)$** :
  Derivatives of $N(x,p) = tanh(z)$ with respect to input x is as follows,

$$\frac{dN}{dx} = \frac{4\sum_{j=1}^{M} w_j T'_{j-1}(x)}{\left(e^{\sum_{j=1}^{M} w_j T_{j-1}(x)} + e^{-\sum_{j=1}^{M} w_j T_{j-1}(x)} \right)^2},\tag{17}$$

and

$$\frac{d^2N}{dx^2} = \frac{4\left[\begin{array}{c} \sum_{j=1}^{M} w_j T''_{j-1}(x) e^{\sum_{j=1}^{M} w_j T_{j-1}(x)} + \sum_{j=1}^{M} w_j T''_{j-1}(x) e^{-\sum_{j=1}^{M} w_j T_{j-1}(x)}, \\ -2\left(\sum_{j=1}^{M} w_j T'_{j-1}(x) \right)^2 e^{\sum_{j=1}^{M} w_j T_{j-1}(x)} + 2\left(\sum_{j=1}^{M} w_j T'_{j-1}(x) \right)^2 e^{-\sum_{j=1}^{M} w_j T_{j-1}(x)} \end{array} \right]}{\left(e^{\sum_{j=1}^{M} w_j T_{j-1}(x)} + e^{-\sum_{j=1}^{M} w_j T_{j-1}(x)} \right)^3}.\tag{18}$$

where w_j denotes the network parameters and $T'_{j-1}(x)$, $T''_{j-1}(x)$ denotes the first and second derivatives of the Chebyshev polynomials. Therefore, from Eq. (11) we have,

$$\frac{dy_t(x,p)}{dx} = A' + 2(x-a)N(x,p) + (x-a)^2\frac{dN}{dx},\tag{19}$$

and

$$\frac{d^2y_t(x,p)}{dx^2} = 2N(x,p) + 4(x-a)\frac{dN}{dx} + (x-a)^2\frac{d^2N}{dx^2}.\tag{20}$$

Also, from Eq. (12) we have,

$$\frac{\partial E(x,p)}{\partial w_j} = \frac{\partial}{\partial w_j}\left[\sum_{i=1}^{n} \frac{1}{2}\left(\frac{d^2y_t(x_i,p)}{dx^2} - f(x_i, y_t(x,p), y'_t(x,p)) \right) \right].\tag{21}$$

Finally, we can use the convergent ChNN results in Eq. (11) to obtain the approximate solutions.

4. Numerical results

In this section, we consider classical Van der Pol, Duffing-Van der Pol and forced Van der Pol-Duffing equations to show the effectiveness of the proposed method.

4.1. Classical van der Pol equation

The classical Van der Pol equation is as found in [22],

$$\frac{d^2y}{dx^2} + \varepsilon(y^2 - 1)\frac{dy}{dx} + y = 0; \qquad y(0) = \alpha, \ \dot{y}(0) = 0,\tag{22}$$

where y shows the displacement of the periodic solution, α is the amplitude of the oscillations and ε is a classical problem in nonlinear dynamics that models systems with self-sustained oscillations.
The network has been trained for thirty equidistant points an intervals $[0,3]$ for computing the results. Comparison between fourth-fifth order Runge-Kutta (RK45) and Chebyshev neural network results (ChNN) are shown in Table (1) with F(z)=sinh(z), M=5;7, $\alpha = 0.1$ and $\varepsilon = 0.1$. Comparison of absolute errors between ChNN and RK45 methods with F(z)=z; sinh(z); tanh(z), M=5;7, $\alpha = 0.1$, $\varepsilon = 0.1$ are cited in Table (2). Values of weights for ChNN method with F(z)=sinh(z), M=5;7, $\alpha = 0.1$ and $\varepsilon = 0.1$ are listed in Table (3). Numerical results of RK45 and ChNN methods are compared in Fig. (2). Plot of absolute error between RK45 and ChNN solutions are showed in Fig. (3). According to Table (1) the maximum error between RK45 and ChNN methods are 0.19547×10^{-2} and 0.93269×10^{-4} for $M = 5;7$, respectively. From Table (2) the maximum error for active functions is according to the order $\mathbf{Error_{sinh(z)}} > \mathbf{Error_z} > \mathbf{Error_{tanh(z)}}$.

4.2. Duffing-van der Pol equation

Consider the Duffing-van der pol equation [22, 23, 24] as follows,

$$\frac{d^2y}{dx^2} + (\alpha + \beta y^2)\frac{dy}{dx} - \gamma y + \lambda y^3 = 0; \quad y(0) = a, \ \dot{y}(0) = b. \tag{23}$$

By supposing that $\gamma = -1/\beta$, $\alpha = 4/\beta$ and $\beta = 3$, $\lambda = 1$, $a = -0.28868$, $b = 0.12$ the analytical solution should be as follows,

$$\begin{aligned} y(x) \quad = \quad & -0.000026166e^{-4.09188x} - 0.00212777e^{-2.16516x} \\ & -0.0266831e^{-1.06495x} - 0.259843e^{-0.334316x}. \end{aligned}$$

The network has been trained with thirty equidistant points at interval $[0,3]$ for computing the results. Comparison between fourth-fifth order Runge-Kutta (RK45), Homotopy Perturbation Method (HPM), Differential Transform Method (DTM), Exact solution and Chebyshev neural network results (ChNN) are shown in Table (4) when F(z)=sinh(z) and M=5;7. Values of weights for ChNN method when F(z)=sinh(z) and M=5;7 have been listed in Table (5). According Table (4) ChNN results fully agree with all numerical methods especially with the exact solution method.

4.3. Duffing-van der Pol oscillators

Duffing oscillators are formulas whose mathematical expression is assumed in the form of the second-order non-autonomous differential equation [25],

$$\frac{d^2y}{dx^2} + \mu(1-y^2)\frac{dy}{dx} + \alpha y + \beta y^3 = g(f,\omega,t); \quad y(0) = 1, \ \dot{y}(0) = 0, \tag{24}$$

where x stands for the displacement from the equilibrium position, f is the forcing strength and $\mu > 0$ is the damping parameter of the system. $g(f,x,t) = f\cos(\omega t)$, represents the periodic driving function of time with period $T = 2\pi/\omega$, where x is the angular frequency of the driving force. The Van der PolDuffing oscillator equation can be expressed in three main physical situations, single well $\alpha > 0$, $\beta > 0$, double well $\alpha < 0$, $\beta > 0$ and double-hump $\alpha > 0$, $\beta < 0$.

Was trained with thirty equidistant points at interval $[0,3]$ for computing the results. Comparison between fourth-fifth order Runge-Kutta (RK45), Homotopy Analysis Method (HAM) and Chebyshev neural results (ChNN) are shown in Table (6) when F(z)=sinh(z), M=5;7, $\alpha = 0.5$, $\beta = 0.5$, $\mu = 0.1$, $\omega = 0.79$ and $f = 0.5$. Values of weights for ChNN method when F(z)=sinh(z), M=5; 7, $\alpha = 0.5$, $\beta = 0.5$, $\mu = 0.1$, $\omega = 0.79$ and $f = 0.5$ have been listed in Table (7). Numerical results of RK45 and ChNN solutions are compared in Fig. (4). Plot for the absolute errors between RK45 and ChNN solutions are showed in Fig. (5). From Table (6) we conclude that ChNN results are in agreement with both RK45 and HAM numerical methods.

Table (8) presents the comparison between ChNN, RK45 and HAM methods when F(z)=sinh(z), M=5; 7, $\alpha = -0.5$, $\beta = 0.5$, $\mu = 0.1$, $\omega = 0.79$ and $f = 0.5$. Weight values for ChNN method have been listed in Table (9). Comparison of numerical results from RK45 and ChNN methods are shown in Fig. (6). Absolute errors between RK45 and ChNN solutions are shown in Fig. (7). According to Table (9) we see that the ChNN results is in good agreement with both RK45 and HAM numerical methods, specially with the RK45 method.

The network was trained with thirty equidistant points at interval $[0,2]$ for computing the results. Comparison between fourth-fifth order Runge-Kutta (RK45), Homotopy Analysis Method (HAM) and Chebyshev neural results (ChNN) are showed in Table (10) when F(z)=sinh(z), M=5;7, $\alpha = 0.5$, $\beta = -0.5$, $\mu = 0.1$, $\omega = 0.79$ and $f = 0.5$. Values of weights for ChNN method when F(z)=sinh(z), M=5; 7, $\alpha = 0.5$, $\beta = -0.5$, $\mu = 0.1$, $\omega = 0.79$ and $f = 0.5$ have been shown in Table (11). The numerical results of RK45 and ChNN solutions are compared in Fig. (8). Plot of the absolute errors between RK45 and ChNN solutions are shown in Fig. (9). Table (10) shows the agreement between the numerical results of ChNN, RK45 and HAM.

Table 1: Comparison between ChNN and RK45 methods with F(z)=sinh(z), M=5;7, $\alpha = 0.1$ and $\varepsilon = 0.1$ (Example 1).

Time	RK45	M=5 ChNN	Error	M=7 ChNN	Error
0.2	0.097993	0.098160	0.16769e-3	0.097977	0.15885e-4
0.4	0.092001	0.092431	0.43356e-3	0.091966	0.34219e-4
0.6	0.082184	0.082766	0.58671e-3	0.082144	0.39393e-4
0.8	0.068861	0.069416	0.55984e-3	0.068825	0.35519e-4
1.0	0.052497	0.052870	0.37610e-3	0.052466	0.31737e-4
2.0	-0.050742	-0.051060	0.31447e-3	-0.050836	0.93269e-4
3.0	-0.115748	-0.114206	0.15672e-2	-0.115751	0.28131e-4
4.0	-0.075655	-0.074453	0.12192e-2	-0.075567	0.89004e-4
5.0	0.041773	0.040377	0.13804e-2	0.041832	0.59140e-4
6.0	0.131125	0.129160	0.19547e-2	0.131140	0.15862e-4

Table 2: Comparison of absolute errors between ChNN and RK45 with `F(z)=z;sinh(z);tanh(z)`, `M=5;7`, $\alpha = \varepsilon = 0.1$ (Example 1).

M	Error		
	F(z)=z	**F(z)=sinh(z)**	**F(z)=tanh(z)**
5	0.195612e-2	0.197132e-2	0.192589e-2
7	0.946373e-4	0.957182e-4	0.924828e-4

Table 3: Weight values with `F(z)=sinh(z)`, `M=5;7`, $\alpha = 0.1$ and $\varepsilon = 0.1$ (Example 1).

M	w_1	w_2	w_3	w_4	w_5	w_6	w_7
5	-0.038074	-0.014324	0.005759	-0.000482	0.0000123	——	——
7	-0.049832	0.0012465	0.000781	0.000348	-0.000062	0.000003	-0.000001

Table 4: Comparison between ChNN, RK45, HPM, DTM methods and Exact solution with `F(z)=sinh(z)` and `M=5;7` (Example 2).

Time	ChNN		RK45	HPM	DTM	Exact
	M=5	**M=7**				
0.0	-0.288680	-0.288680	-0.288680	-0.288680	-0.288680	-0.288680
0.01	-0.288349	-0.2867983	-0.287474	-0.287483	-0.287485	-0.287483
0.02	-0.286742	-0.2858550	-0.286256	-0.286294	-0.286307	-0.2862939
0.03	-0.285051	-0.2848782	-0.285026	-0.285111	-0.285144	-0.285111
0.04	-0.283094	-0.2839268	-0.283784	-0.283935	-0.283998	-0.283935
0.05	-0.281199	-0.2829547	-0.282531	-0.280447	-0.282869	-0.2827658
0.06	-0.279701	-0.2819825	-0.281266	-0.279298	-0.281756	-0.2816032
0.07	-0.278572	-0.2810342	-0.279989	-0.278146	-0.280661	-0.280447
0.08	-0.277540	-0.2800903	-0.278701	-0.277018	-0.279519	-0.279298
0.09	-0.276297	-0.2791306	-0.277401	-0.278155	-0.278520	-0.278155
1.0	-0.274776	-0.2781893	-0.276090	-0.277018	-0.277476	-0.277018

Table 5: Weight values with `F(z)=sinh(z)` and `M=5;7` (Example 2).

M	w_1	w_2	w_3	w_4	w_5	w_6	w_7
5	-80872.0472	50193.8336	-0.00001	16605.9393	-25665.4792	———	———
7	-0.049832	0.0012465	0.000781	0.000348	-0.000062	0.000003	-0.000001

Table 6: Comparison between ChNN, RK45 and HAM methods with `F(z)=sinh(z)`, `M=5; 7`, $\alpha = 0.5$, $\beta = 0.5$, $\mu = 0.1$, $\omega = 0.79$ and $f = 0.5$ (Example 3).

Time	ChNN		RK45	HAM
	M=5	M=7		
0.2	0.989364	0.990077	0.990045	0.990045
0.4	0.959024	0.960757	0.960702	0.960702
0.6	0.911465	0.913482	0.913415	0.913415
0.8	0.849144	0.850341	0.850249	0.859249
1.0	0.774289	0.773644	0.773522	0.773522
2.0	0.260669	0.247835	0.247739	0.247739
3.0	-0.456965	-0.480696	-0.480716	-0.480716

Table 7: Weight values with `F(z)=sinh(z)`, `M=5; 7`, $\alpha = 0.5$, $\beta = 0.5$, $\mu = 0.1$, $\omega = 0.79$ and $f = 0.5$ (Example 3).

M	w_1	w_2	w_3	w_4	w_5	w_6	w_7
5	-0.21932215	-0.02586752	0.02494517	-0.00444285	0.00025808	———	———
7	-0.22395577	-0.01880817	0.02176276	-0.03609309	0.00013547	0.00000927	-0.00000027

Table 8: Comparison between ChNN, RK45 and HAM methods with `F(z)=sinh(z)`, M=5; 7, $\alpha = -0.5$, $\beta = 0.5$, $\mu = 0.1$, $\omega = 0.79$ and $f = 0.5$ (Example 3).

Time	ChNN		RK45	HAM
	M=5	**M=7**		
0.2	1.008519	1.0102725	1.009945	1.009945
0.4	1.035947	1.0396684	1.039114	1.039114
0.6	1.081721	1.0860922	1.085449	1.085447
0.8	1.141831	1.1462449	1.145385	1.145382
1.0	1.210037	1.2149567	1.213778	1.213783
2.0	1.419977	1.4298385	1.429818	1.429493
3.0	1.036249	1.0284452	1.029417	1.031066

Table 9: Weight values with `F(z)=sinh(z)`, M=5; 7, $\alpha = -0.5$, $\beta = 0.5$, $\mu = 0.1$, $\omega = 0.79$ and $f = 0.5$ (Example 3).

M	w_1	w_2	w_3	w_4	w_5	w_6	w_7
5	0.10862971	0.17126788	-0.08088946	0.00990175	0.00990175	———	———
7	0.32424439	-0.15155358	0.06325686	-0.02701543	0.00473990	-0.00034542	0.00000813

Table 10: Comparison between ChNN, RK45 and HAM methods with `F(z)=sinh(z)`, M=5; 7, $\alpha = 0.5$, $\beta = -0.5$, $\mu = 0.1$, $\omega = 0.79$ and $f = 0.5$ (Example 3).

Time	ChNN		RK45	HAM
	M=5	**M=7**		
0.1	1.002789	1.002595	1.002501	1.002500
0.2	1.010651	1.010240	1.010012	1.010012
0.5	1.062186	1.063531	1.063007	1.063007
1.0	1.254493	1.261717	1.260394	1.260394
1.5	1.627465	1.643387	1.640771	———
2.0	2.381650	2.424097	2.417826	———

Table 11: Weight values with `F(z)=sinh(z)`, M=5; 7, $\alpha = 0.5$, $\beta = -0.5$, $\mu = 0.1$, $\omega = 0.79$ and $f = 0.5$ (Example 3).

M	w_1	w_2	w_3	w_4	w_5	w_6	w_7
5	0.44260284	-0.31126987	0.15490507	-0.03905212	0.00463758	———	———
7	0.43220189	-0.30483037	0.19299251	-0.08183546	0.02396069	-0.00398242	0.00031131
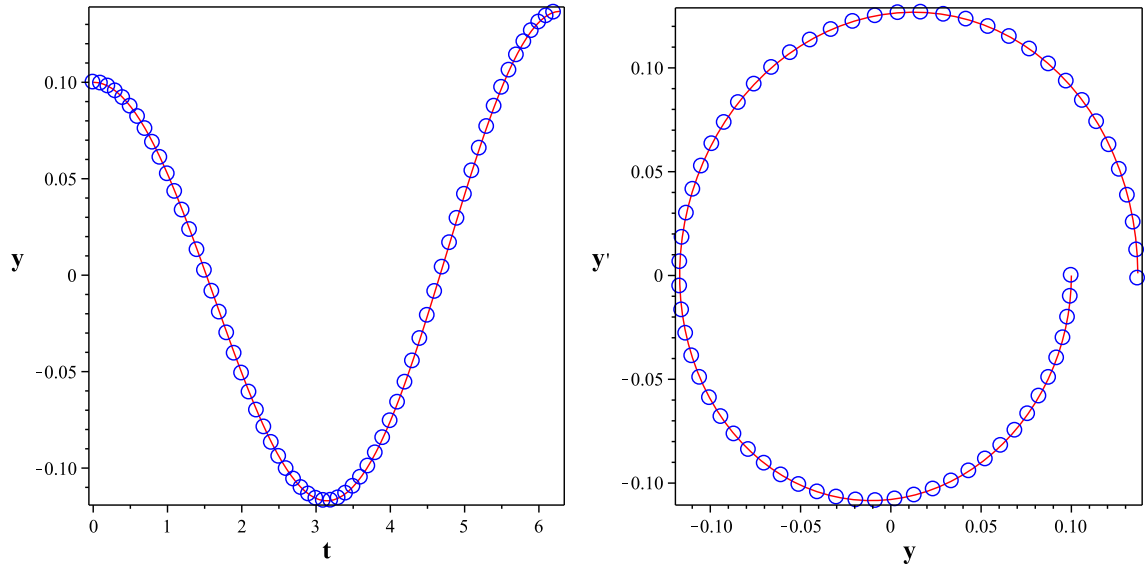
Figure 2: Plot of numerical solutions using RK45 and ChNN (Example 1).
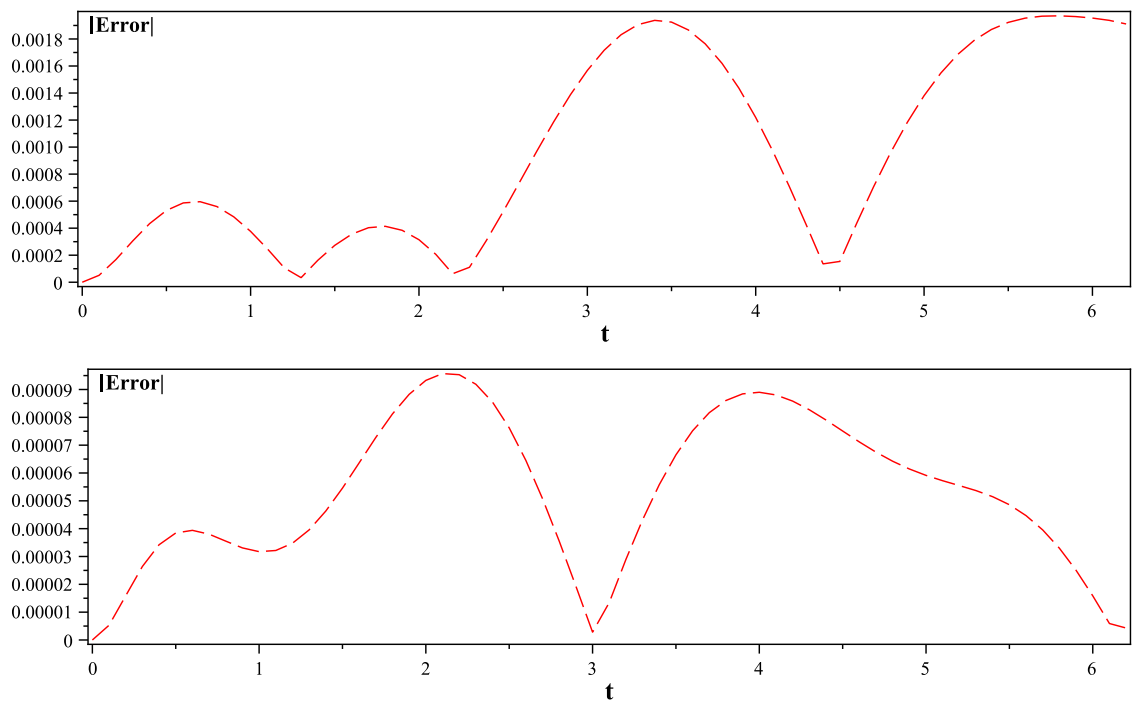
Figure 3: Plot of absolute error between RK45 and ChNN solutions (Example 1).
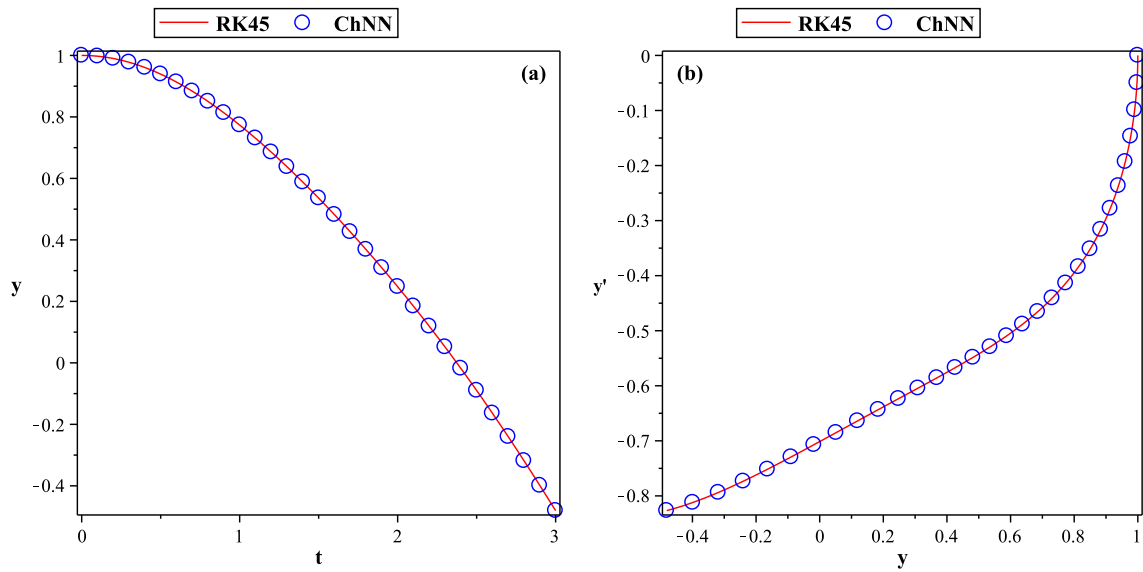
Figure 4: Plot of numerical solutions using RK45 and ChNN solutions when `F(z)=sinh(z)`, `M=5; 7`, $\alpha = 0.5$, $\beta = 0.5$, $\mu = 0.1$, $\omega = 0.79$ and $f = 0.5$ (Example 2).
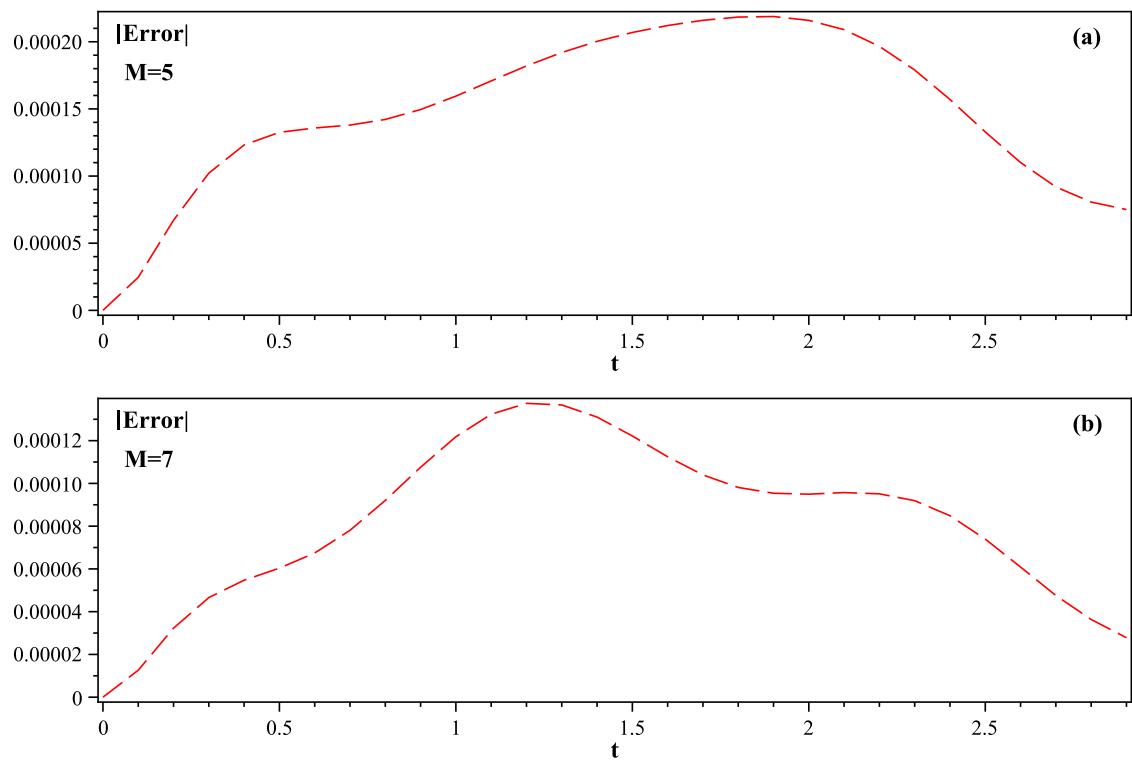
Figure 5: Plot of absolute error between RK45 and ChNN solutions when `F(z)=sinh(z)`, `M=5; 7`, $\alpha = 0.5$, $\beta = 0.5$, $\mu = 0.1$, $\omega = 0.79$ and $f = 0.5$ (Example 2).
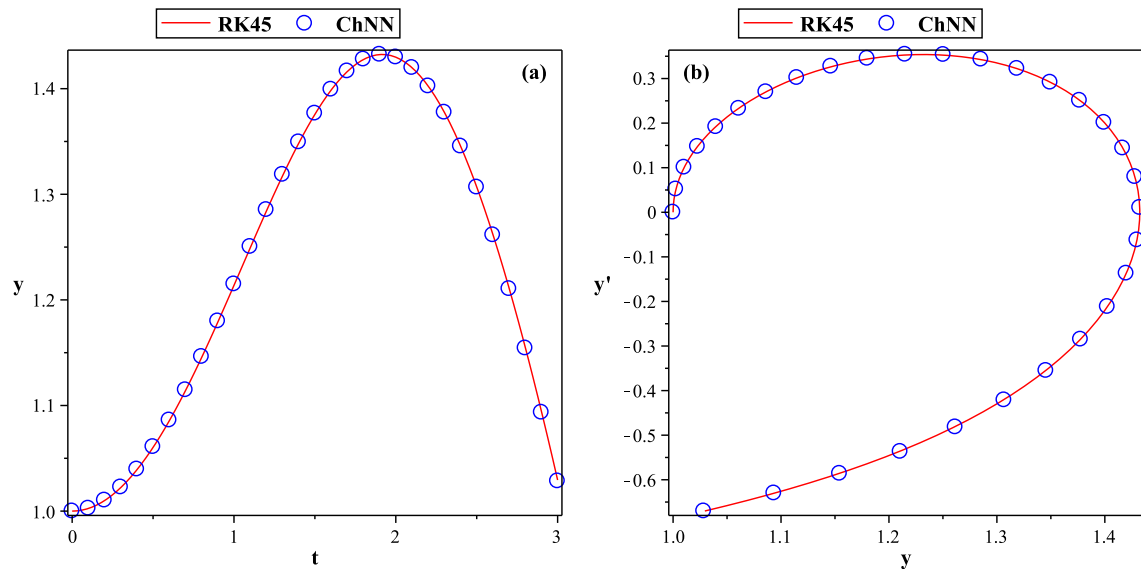
Figure 6: Plot of numerical solutions using RK45 and ChNN solutions when `F(z)=sinh(z)`, `M=5; 7`, $\alpha = -0.5$, $\beta = 0.5$, $\mu = 0.1$, $\omega = 0.79$ and $f = 0.5$ (Example 3).
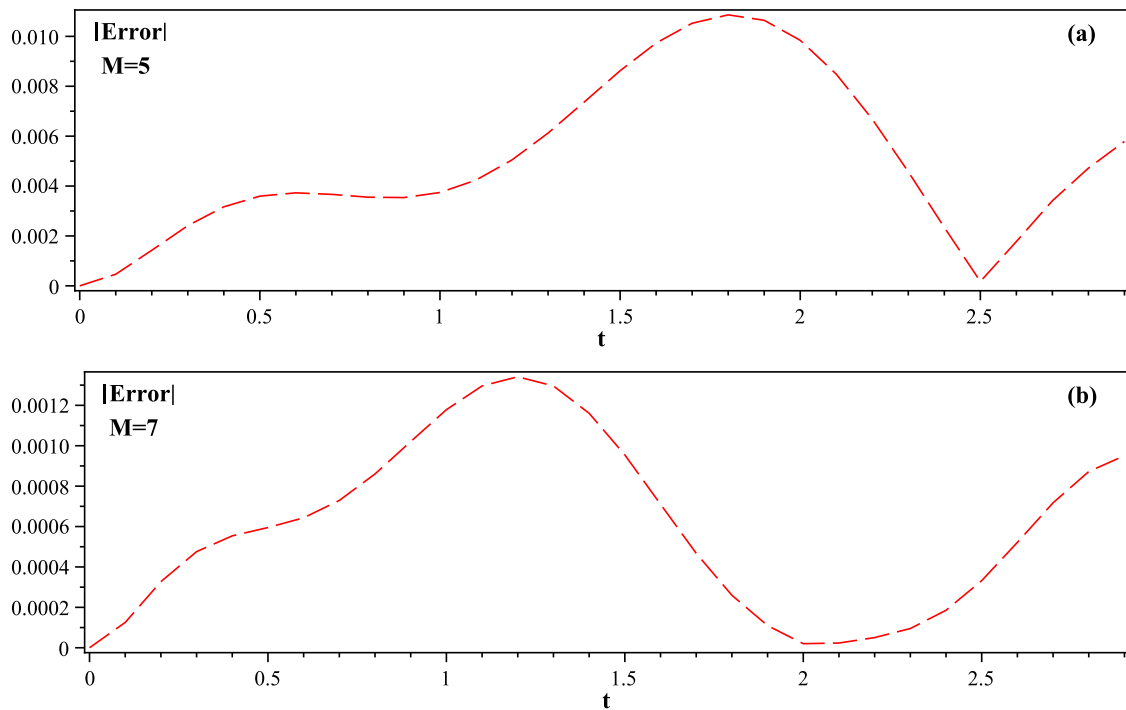
Figure 7: Plot of absolute error between RK45 and ChNN solutions when `F(z)=sinh(z)`, `M=5; 7`, $\alpha = -0.5$, $\beta = 0.5$, $\mu = 0.1$, $\omega = 0.79$ and $f = 0.5$ (Example 3).
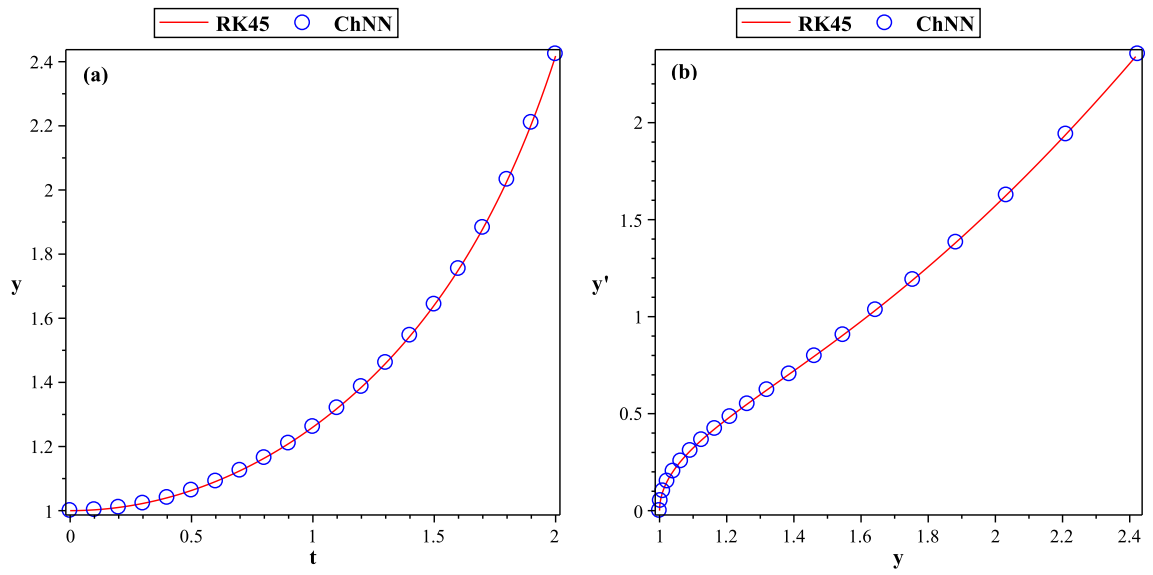
Figure 8: Plot of numerical solutions using RK45 and ChNN solutions when `F(z)=sinh(z)`, `M=5; 7`, $\alpha = 0.5$, $-\beta = 0.5$, $\mu = 0.1$, $\omega = 0.79$ and $f = 0.5$ (Example 3).
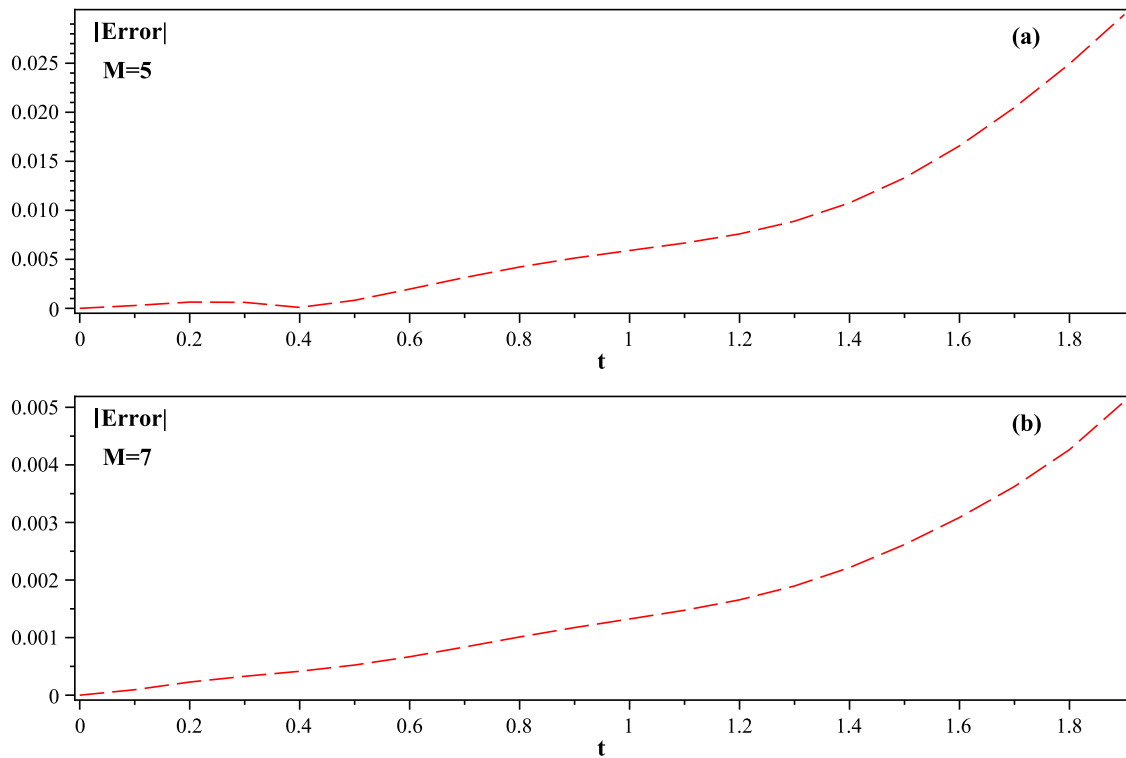
Figure 9: Plot of absolute error between RK45 and ChNN solutions when `F(z)=sinh(z)`, `M=5; 7`, $\alpha = 0.5$, $\beta = -0.5$, $\mu = 0.1$, $\omega = 0.79$ and $f = 0.5$ (Example 3).

5. Conclusions

The Chebyshev Neural Network (ChNN) model was applied to to solve single-well, double-well and double-hump Van der Pol-Dufing equations. A single layer Chebyshev Neural Network (ChNN) model is considered as a solution for the difficulties of this type of equations. For optimizing weight values, the gradient of network outputs with respect to their inputs are considered. The numerical results obtained from ChNN model have been compared with the analytical, Homotopy Perturbation Method (HPM), Homotopy Analysis Method (HAM) and Differential Transform Method (DTM) solutions. The errors obtained showed that the ChNN solutions has excellent agreement with all numerical results from exact solutions or other numerical methods. Comparisons of the obtained solutions with existing numerical results showed that this method is a capable tool for solving this kind of nonlinear problems and also extremely powerful and easy to implement, computationally efficient and straight forward.
0.8

References

[1] B. Van der Pol, "A theory of the amplitude of free and forced triode vibrations," *Radio Review*, vol. 1, no. 1920, pp. 701–710, 1920.

[2] A. Kimiaeifar, A. Saidi, G. Bagheri, M. Rahimpour, and D. Domairry, "Analytical solution for van der pol–duffing oscillators," *Chaos, Solitons & Fractals*, vol. 42, no. 5, pp. 2660–2666, 2009.

[3] A. Kimiaeifar, A. Saidi, A. Sohouli, and D. Ganji, "Analysis of modified van der pols oscillator using hes parameter-expanding methods," *Current Applied Physics*, vol. 10, no. 1, pp. 279–283, 2010.

[4] N. A. Khan, M. Jamil, S. A. Ali, and N. A. Khan, "Solutions of the force-free duffing-van der pol oscillator equation," *International Journal of Differential Equations*, vol. 2011, 2011.

[5] Y. Chen and J. Liu, "Uniformly valid solution of limit cycle of the duffing–van der pol equation," *Mechanics Research Communications*, vol. 36, no. 7, pp. 845–850, 2009.

[6] H. Molaei and S. Kheybari, "A numerical solution of classical van der pol-duffing oscillator by hes parameter-expansion method," *Int. J. Contemp. Math. Sciences*, vol. 8, no. 15, pp. 709–714, 2013.

[7] S. S. Motsa and P. Sibanda, "A note on the solutions of the van der pol and duffing equations using a linearisation method," *Mathematical Problems in Engineering*, vol. 2012, 2012.

[8] S. Mukherjee, B. Roy, and S. Dutta, "Solution of the duffing–van der pol oscillator equation by a differential transform method," *Physica Scripta*, vol. 83, no. 1, p. 015006, 2011.

[9] G. M. Mahmoud, A. A. Farghaly, T. M. Abed-Elhameed, S. A. Aly, and A. A. Arafa, "Dynamics of distributed-order hyperchaotic complex van der pol oscillators and their synchronization and control," *The European Physical Journal Plus*, vol. 135, no. 1, pp. 1–16, 2020.

[10] S. Mungkasi, "Numerical verification of the orders of accuracy of truncated asymptotic expansion solutions to the van der pol equation," *Journal of Mathematical Chemistry*, pp. 1–8, 2020.

[11] M. Kumar and P. Varshney, "Numerical simulation of van der pol equation using multiple scales modified lindstedt–poincare method," *Proceedings of the National Academy of Sciences, India Section A: Physical Sciences*, pp. 1–11, 2020.

[12] A. S. Soomro, G. A. Tularam, and M. M. Shaikh, "A comparison of numerical methods for solving the unforced van der pols equation," *Mathematical Theory and Modeling*, vol. 3, no. 2, pp. 66–77, 2013.

[13] Q. Bi, "Dynamical analysis of two coupled parametrically excited van der pol oscillators," *International Journal of Non-Linear Mechanics*, vol. 39, no. 1, pp. 33–54, 2004.

[14] L. Liu, E. H. Dowell, and K. C. Hall, "A novel harmonic balance analysis for the van der pol oscillator," *International Journal of Non-Linear Mechanics*, vol. 42, no. 1, pp. 2–12, 2007.

[15] M. Belhaq and S. Mohamed Sah, "Fast parametrically excited van der pol oscillator with time delay state feedback," *International Journal of Non-Linear Mechanics*, vol. 43, no. 2, pp. 124–130, 2008.

[16] P. Perlikowski, A. Stefanski, and T. Kapitaniak, "Discontinuous synchrony in an array of van der pol oscillators," *International Journal of Non-Linear Mechanics*, vol. 45, no. 9, pp. 895–901, 2010.

[17] P. Ramana and B. Raghu Prasad, "Modified adomian decomposition method for van der pol equations," *International Journal of Non-Linear Mechanics*, 2014.

[18] S. S. Chaharborj, S. Chaharborj, and Y. Mahmoudi, "Study of fractional order integro-differential equations by using chebyshev neural network," *J. Math. Stat*, vol. 13, no. 1, pp. 1–13, 2017.

[19] S. Mall and S. Chakraverty, "Chebyshev neural network based model for solving lane–emden type equations," *Applied Mathematics and Computation*, vol. 247, pp. 100–114, 2014.

[20] ——, "Numerical solution of nonlinear singular initial value problems of emden–fowler type using chebyshev neural network method," *Neurocomputing*, vol. 149, pp. 975–982, 2015.

[21] S. Hoda and H. Nagla, "Neural network methods for mixed boundary value problems," *International Journal of Nonlinear Science*, vol. 11, no. 3, pp. 312–316, 2011.

[22] N. A. Khan, M. Jamil, S. A. Ali, and N. A. Khan, "Solutions of the force-free duffing-van der pol oscillator equation," *International Journal of Differential Equations*, vol. 2011, 2011.

[23] V. Chandrasekar, M. Senthilvelan, and M. Lakshmanan, "New aspects of integrability of force-free duffing–van der pol oscillator and related nonlinear systems," *Journal of Physics A: Mathematical and General*, vol. 37, no. 16, p. 4527, 2004.

[24] N. A. Khan, A. Ara, S. A. Ali, and A. Mahmood, "Analytical study of navier-stokes equation with fractional orders using he's homotopy perturbation and variational iteration methods," *International Journal of Nonlinear Sciences and Numerical Simulation*, vol. 10, no. 9, pp. 1127–1134, 2009.

[25] A. Kimiaeifar, A. Saidi, G. Bagheri, M. Rahimpour, and D. Domairry, "Analytical solution for van der pol–duffing oscillators," *Chaos, Solitons & Fractals*, vol. 42, no. 5, pp. 2660–2666, 2009.